

Article

Impacts of Climate Alteration on the Hydrology of the Yarra River Catchment, Australia Using GCMs and SWAT Model

Sushil K. Das ¹, Amimul Ahsan ^{2,3}, Md. Habibur Rahman Bejoy Khan ²,
Muhammad Atiq Ur Rehman Tariq ^{1,4}, Nitin Muttill ^{1,4,*} and Anne W. M. Ng ^{5,*}

¹ College of Engineering and Science, Victoria University, P.O. Box 14428, Melbourne, VIC 8001, Australia; sushil.das@live.vu.edu.au (S.K.D.); atiq.tariq@yahoo.com (M.A.U.R.T.)

² Department of Civil and Environmental Engineering, Islamic University of Technology, Gazipur 1704, Bangladesh; ahsan.upm2@gmail.com (A.A.); cee.bejoy@iut-dhaka.edu (M.H.R.B.K.)

³ Department of Civil and Construction Engineering, Swinburne University of Technology, Melbourne, VIC 3122, Australia

⁴ Institute for Sustainable Industries and Liveable Cities, Victoria University, P.O. Box 14428, Melbourne, VIC 8001, Australia

⁵ College of Engineering, Information Technology and Environment, Charles Darwin University, Ellengowan Dr, Brinkin, NT 0810, Australia

* Correspondence: nitin.muttill@vu.edu.au (N.M.); anne.ng@cdu.edu.au (A.W.M.N.); Tel.: +61-3-9919-4251 (N.M.); +61-8-8946-6230 (A.W.M.N.)

Abstract: A rigorous evaluation of future hydro-climatic changes is necessary for developing climate adaptation strategies for a catchment. The integration of future climate projections from general circulation models (GCMs) in the simulations of a hydrologic model, such as the Soil and Water Assessment Tool (SWAT), is widely considered as one of the most dependable approaches to assess the impacts of climate alteration on hydrology. The main objective of this study was to assess the potential impacts of climate alteration on the hydrology of the Yarra River catchment in Victoria, Australia, using the SWAT model. The climate projections from five GCMs under two Representative Concentration Pathway (RCP) scenarios—RCP 4.5 and 8.5 for 2030 and 2050, respectively—were incorporated into the calibrated SWAT model for the analysis of future hydrologic behaviour against a baseline period of 1990–2008. The SWAT model performed well in its simulation of total streamflow, baseflow, and runoff, with Nash–Sutcliffe efficiency values of more than 0.75 for monthly calibration and validation. Based on the projections from the GCMs, the future rainfall and temperature are expected to decrease and increase, respectively, with the highest changes projected by the GFDL-ESM2M model under the RCP 8.5 scenario in 2050. These changes correspond to significant increases in annual evapotranspiration (8% to 46%) and decreases in other annual water cycle components, especially surface runoff (79% to 93%). Overall, the future climate projections indicate that the study area will become hotter, with less winter–spring (June to November) rainfall and with more water shortages within the catchment.

Keywords: climate alteration impacts; hydrology; GCMs; SWAT; Yarra River; Australia



Citation: Das, S.K.; Ahsan, A.; Khan, M.H.R.B.; Tariq, M.A.U.R.; Muttill, N.; Ng, A.W.M. Impacts of Climate Alteration on the Hydrology of the Yarra River Catchment, Australia Using GCMs and SWAT Model. *Water* **2022**, *14*, 445. <https://doi.org/10.3390/w14030445>

Academic Editors: Alban Kuriqi and Rafael J. Bergillos

Received: 8 December 2021

Accepted: 27 January 2022

Published: 1 February 2022

Publisher's Note: MDPI stays neutral with regard to jurisdictional claims in published maps and institutional affiliations.



Copyright: © 2022 by the authors. Licensee MDPI, Basel, Switzerland. This article is an open access article distributed under the terms and conditions of the Creative Commons Attribution (CC BY) license (<https://creativecommons.org/licenses/by/4.0/>).

1. Introduction

The alteration of climate has occurred since industrialization due to greenhouse gas pollution and rapid advancements in technology [1]. According to the recent Intergovernmental Panel on Climate Change (IPCC) report, the global average surface temperature rose by 0.85 °C between 1880 and 2012 [2]. Since 1910, the average temperature of Australia has increased by 1.4 °C, resulting in extreme heat events and a decline in rainfall in the southern and eastern regions of the continent [3]. Climate alteration likely impacts catchment hydrology due to changes in rainfall, temperature, and atmospheric CO₂ levels. Changes in rainfall volume and variability are anticipated to have the most significant

impact on catchment hydrology, resulting in seasonal timing shifts and changes in water yields [4]. In addition, temperature variation will have an impact on the growing seasons of trees and plants, and changes may also be seen in the hydrologic cycle through increased evapotranspiration [5].

The hydrologic changes will impact nearly every aspect of human life. For example, larger channel spillways and drainage canals will be necessary as extreme rainfall events are expected to increase in intensity and frequency. In contrast, more water supply storage will be required as runoff is expected to reduce. Water's enormous significance in both society and nature emphasizes the importance of acknowledging how a change in the global climate may affect a basin's water resource.

The magnitude of climate alteration impacts and their adverse effects is difficult to predict with accuracy. Integrating future climate projections from general circulation models (GCMs) into hydrologic model simulations is considered as one of the most reliable methods for assessing the effects of climate alteration on water resources [6]. However, the output resolution of GCMs is too coarse to load in the hydrologic models [7]. Due to this, several downscaling methods, such as statistical and dynamic downscaling, have been developed to transform climate data from a coarser to a finer resolution [8]. Furthermore, climate scenarios have evolved steadily from plain hypothetical situations to more real-life situations, such as the Special Report on Emissions Scenarios (A1, A2, B1, B2) and the recent Representative Concentration Pathways (RCPs; RCP2.6, RCP4.5, RCP6.0, and RCP8.5) developed by the IPCC in 2001 and 2013, respectively. Li and Fang [9], as well as CSIRO and BoM [10], have provided detailed information on GCMs, downscaling methods, and climate scenarios.

Lumped parameter conceptual hydrological models are commonly used to simulate runoff under climate alterations, especially in Australian conditions [11,12], for example, the Australian water balance model (AWBM) [13] and SIMHYD [14] models. However, physics-based models are not suitable for various Australian catchment areas due to a lack of model development and assessment data [15]. Howe et al. [16] used a group of 13 GCMs and the AWBM model to assess the impact of climate change on Melbourne's water resources. Potter et al. [11] used the SIMHYD model and an ensemble of 42 GCMs for hydroclimate projections of Victoria. They found a 4–6% increase in potential evapotranspiration (PET) by 2040 and a 6–10% increase by 2065, driven mainly by increasing temperatures. Moreover, the decrease in runoff will be greater than 20% and 40% by 2040 and 2065, respectively. Post et al. [17] discovered similar climate alteration impacts on runoff in south-eastern Australia using the SIMHYD model and an ensemble of 15 GCMs. Nguyen et al. [18] used a group of supportive SWAT-SALMO models to guess the daily patterns of nutrient flow in the Millbrook catchment reservoir systems of south Australia, and they discovered significant eutrophication impacts in the reservoir due to future climate alteration.

Physics-based models, such as SWAT, are more suitable for the precise simulation of temporal and spatial arrays in surface runoff, chemicals, and their connected flow path; however, a considerable amount of data and processing are required by the model [19,20]. Gassman et al. [21] examined the SWAT model for climate variation impact studies with various GCMs and concluded that the SWAT model is a versatile and vigorous tool for simulating a wide range of catchment processes. The impacts of climate alteration can be directly simulated in SWAT by taking into account: (1) the effects of higher CO₂ concentrations in the atmosphere based on plant growth and transpiration and (2) changes in climatic inputs [21]. SWAT includes methods for explaining how CO₂ concentration, rainfall, temperature, and humidity affect plant growth, Evapotranspiration (ET), snow, and runoff generation, and is frequently used to explore the effects of climate alteration [22]. Several studies have recently been conducted using the SWAT model to assess climate alteration impacts on the hydrology of catchments around the world [6,18,23–27]. Notably, Rajib and Merwade [25] used the SWAT model to assess the impact of land use change in the upper Mississippi River basin at monthly intervals. Sunde et al. [27] also used the SWAT model to assess the potential effects of climate alteration on streamflow processes

in a mixed-use catchment in the US on a seasonal time scale for the mid-21st century (2040–2069) and the late 21st century (2070–2100).

Australia is historically the driest inhabited continent, and several studies have shown that the climate in many parts of the country (for example southeast Australia, where our study area is located) is changing rapidly when compared to the long-term historical average [3]. The country is predicted to face more frequent hot and dry days in the future, along with increased rainfall intensity during extreme storm events [16]. This climate change has a massive impact on the catchment's agriculture, freshwater supply, and industrial sectors, necessitating a systematic assessment of future hydro-climatic impacts.

The aims of the research undertaken in this study are as follows:

- a. To assess the potential effects of future climate alteration on the hydrology of the middle Yarra River catchment in Victoria, Australia. The SWAT model was chosen for the assessment of future hydrologic behaviour in 2030 and 2050 against a baseline period of 1990–2008 using the application-ready downscaled data of five Coupled Model Intercomparison Project phase 5 (CMIP5) GCMs (ACCESS1-0, CanESM2, CNRM-CM5, GFDL-ESM2M, and MIROC5) under the scenarios of RCP 4.5 and RCP 8.5. To date, no work has been found in the literature to the best of our knowledge that assesses future climate alterations and their impacts on the hydrology of the Yarra River catchment.
- b. To apply the SWAT model in the context of Australian catchments, where many available data are sparse. Because of this, only a few applications of the SWAT model that undertake future climate alteration studies are found in Australia [18,28]. As far as the authors are aware, this is one of the first studies that has implemented the SWAT model to study the middle Yarra River catchment.

The results from this research could be utilized by ecologists and water managers to develop an extensive water resources management plan for the Yarra River catchment. This will support an integrated catchment management plan with better strategies by also considering the environmental aspects of the catchment. The paper is structured as follows. The following section presents the methodology used in this study. It is then followed by a section presenting the results and discussion, and the conclusions drawn from this study are finally presented in the last section.

2. Methodology

2.1. Location

The Yarra River in the state of Victoria in Australia is a potential source of high-quality potable water, especially the forested upper reach, with a total catchment area of about 4000 km² [29]. The catchment is sub-divided into three distinct portions—the lower, middle, and upper Yarra divisions—according to its land use pattern. The land use patterns in the lower and upper divisions are mainly urban and forest, respectively, whereas that in the middle division is mainly agricultural. The Middle Yarra Division (MYD), which covers 1511 km² of the area, was chosen for this study (location shown in Figure 1).

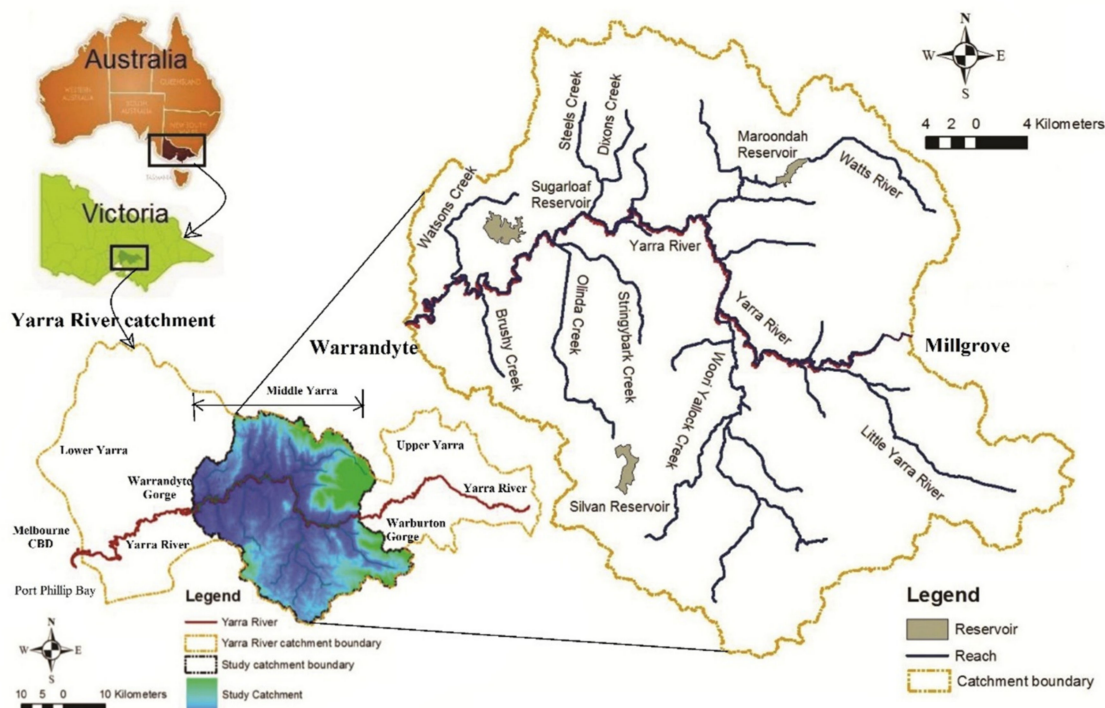


Figure 1. Location of the middle Yarra division [30,31].

2.2. Input Data in Modelling

The ArcSWAT interface of the SWAT2005 model developed by the USDA-ARS was utilized in this study; for the ArcSWAT users' guide and the development of the SWAT model, please refer to Winchell et al. [32] and Arnold et al. [19], respectively. SWAT includes a powerful sensitivity, autocalibration, and uncertainty analysis tool. As a result, many researchers have recommended using this model, especially in agricultural catchments for long-term simulations [21,33]. In addition, SWAT requires extensive data to develop the model. In the study area, information on erosion, soil properties, spatially referenced land use, and data on crop management practices were relatively sparse. Table 1 presents all required input data for the SWAT model. Figure 2 depicts the digital input maps and the climate and streamflow data monitoring stations.

Table 1. Data sources for the SWAT model.

Data	Sources
Digital elevation model (DEM)	ASTER 30 m GDEM, jointly developed by The Ministry of Economy, Trade, and Industry (METI) of Japan and the United States National Aeronautics and Space Administration (NASA), (http://asterweb.jpl.nasa.gov/gdem.asp , (accessed on 26 January 2022)).
Soil	Atlas of Australian Soils from the Department of Agriculture, Fisheries and Forestry, and CSIRO (http://www.asris.csiro.au , (accessed on 18 November 2021)).
Land use	Australian Bureau of Agricultural and Resource Economics and Sciences (50 m grid raster data for 1997 to May 2006) (http://www.agriculture.gov.au/abares/aclump/land-use , (accessed on 26 January 2022)).
Climate	SIL0 climate database (http://www.longpaddock.qld.gov.au/silo , (accessed on 15 October 2021)) and Bureau of Meteorology data for 16 precipitation/rainfall stations, and four weather stations (temperature max and min, solar radiation, wind speed, and relative humidity).
Streamflow	Melbourne Water (http://www.melbournewater.com.au/water-data-and-education/rainfall-and-river-levels#/, (accessed on 26 January 2022)) for daily time series data at Warrandyte (outlet of the MYD) and at Millgrove.
Crop management practices	Australian Bureau of Statistics (http://www.abs.gov.au , (accessed on 14 September 2021)), Melbourne Water, and the Department of Environment and Primary Industries (http://www.depi.vic.gov.au/, (accessed on 14 September 2021)) for data including tillage practices, cropping seasons, and irrigation rate.

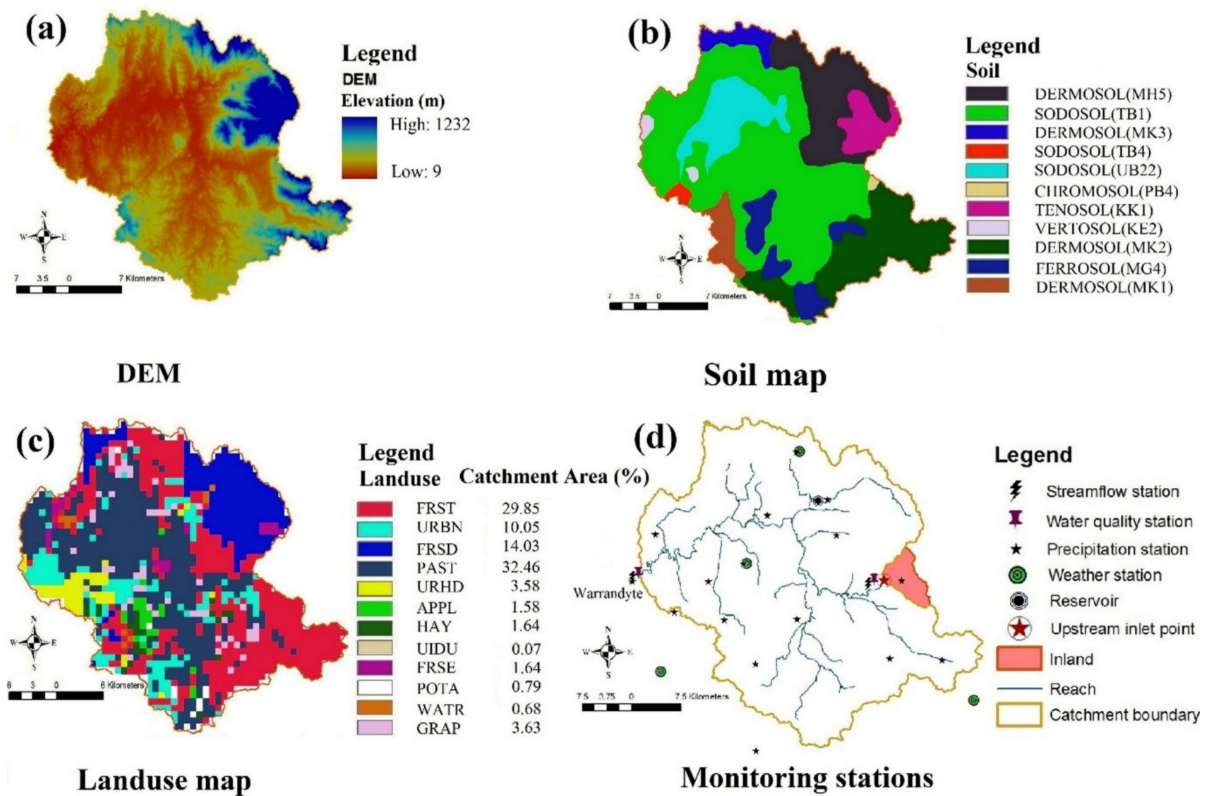


Figure 2. Spatial input maps (a) DEM, (b) Soil map, (c) Landuse map and (d) monitoring stations for SWAT model in the MYD [30,31].

For this study, the SWAT model used ASTER 30m GDEM, as shown in Figure 2a. The soil names in Figure 2b are represented with the dominant principal profile form shown in brackets as per the ASC (Australian Soil Classification) and Factual key methods [34,35]. Sodosol (54%) and dermosol (35%) were the main soil in the catchment. For two layers of the soil, various soil properties were available. Figure 2c illustrates the comprehensive land use forms in the MYD, where pasture accounted for approximately 32% of the total region. The SWAT model generated land use classes for the MYD following the compatibility of the model guidelines, as the model had pre-defined land use forms for creating links with land use maps [32].

The climate data were collected from 1980 to 2008. Figure 3 shows the MYD’s average monthly temperature and rainfall. In September, the highest rainfall occurred, whereas the lowest occurred in February. The highest average temperature varied from 11.40 °C in July to 25.30 °C in February, whereas the lowest varied from 4.40 °C in July to 12.30 °C in February. Figure 4 shows the most acute drought in the recent past that occurred in the MYD, and is denoted by a sudden decline in annual average rainfall (from 1140 to 922 mm) in the beginning of 1997 (known as the Millennium Drought). Such droughts necessitate the need for future climate change impact studies on the catchment’s hydrology.

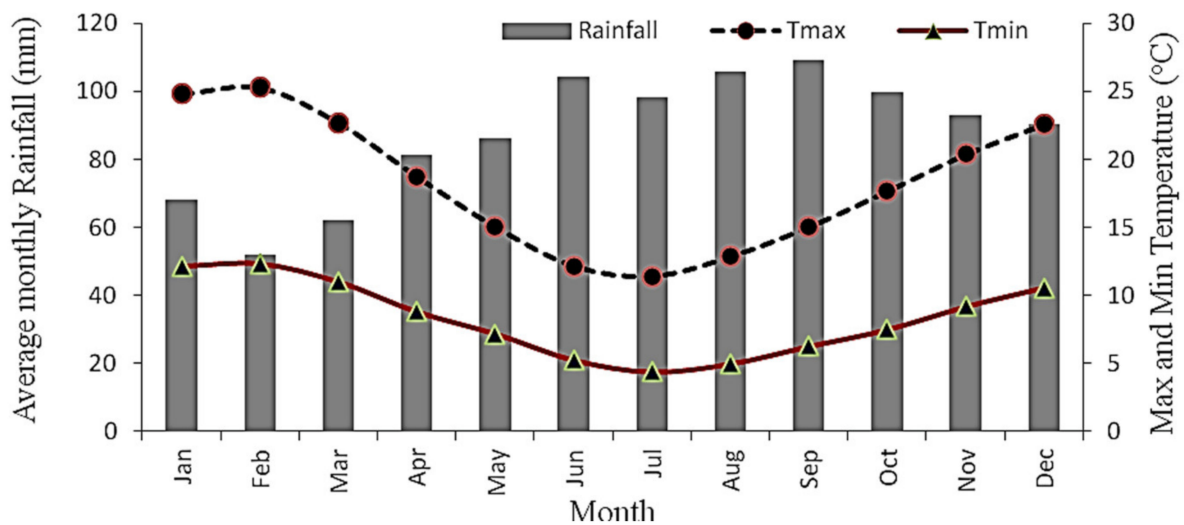


Figure 3. Average monthly rainfall and temperature (max and min) in the MYD [30].

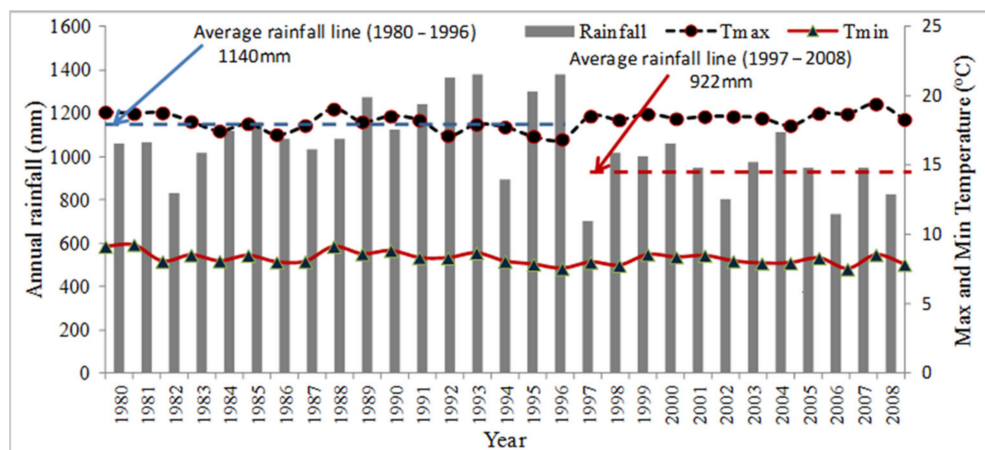


Figure 4. Annual rainfall and temperature (max and min) in the MYD [30].

The accurate representation of surface and subsurface hydrological processes can be achieved by calibrating the baseflow, surface runoff, and total streamflow. Baseflow was separated in this study using the “Baseflow Filter Program” which is an automated digital filter-based software [36,37]. The baseflow estimation indicated that the MYD’s baseflow was about 75% of the total streamflow. Streamflow data from the Millgrove station (see Figure 1) was used to add the upper division’s flow of the Yarra River into the MYD using the “upstream inlet point” function of the SWAT model (refer to Figure 2d to see the location of the upstream inlet point).

2.3. SWAT Model: Formulation, Sensitivity Analysis, Calibration, and Validation

As per the guidelines of Winchell et al. [32], all the spatial datasets and input files were prepared and used to develop the SWAT model. ArcGIS was used to process and prepare the spatial datasets and their input files along with other readily available tools, such as Microsoft Excel. In the model, the MYD was divided into 51 sub-catchments and 431 hydrological response units (HRUs), each with its own distinctive combination of land use, soil form, and slope. To estimate runoff, PET and channel routing in the model, curve number (CN), Penman–Monteith, and Muskingum methods were used respectively.

The sensitivity and auto-calibration tool of the SWAT model [38] was utilized at Warrandyte (the MYD outlet in Figure 2d) for model sensitivity and calibration analysis.

SWAT has a total of 26 streamflow parameters. Each parameter is assigned an initial value from the default lower and higher limit during the model setup, following the study area's climate, soil, land-use, and topography. During the calibration process, the model's output variables are modified by assessing the initial values of the parameters that are found to be sensitive, while the other parameters remain unchanged. The LH-OAT (Latin-hypercube and one-factor-at-a-time) approaches are utilized for all streamflow parameters in the sensitivity analysis of the SWAT model. Then, the ParaSol (SCE-UA) auto-calibration analysis is accomplished using the most sensitive streamflow parameters. In addition, in the SWAT model, the manual tuning of the runoff and baseflow-related parameters is performed for runoff and baseflow calibration.

In addition to the visual/graphic approaches, the Nash–Sutcliffe efficiency (NSE), percent bias (PBIAS), and the ratio of the root mean square error to the standard deviation of measured data (RSR) were used in the model evaluation, as recommended by Moriasi et al. [39]. The optimal RSR and P_x values were 0, and negative and positive PBIAS values implied overprediction and underprediction in model output, respectively. According to Moriasi et al. [39], a satisfactory model output has NSE > 0.50%, RSR > 0.70%, and PBIAS > 25% in a monthly time step for streamflow. In addition, the coefficient of determination (R²) was used in evaluating the model output.

2.4. General Circulation Models (GCMs), Future Climate Scenarios, and Projection Data

According to the recent IPCC report, there are more than 40 GCMs developed around the world. CSIRO and BoM [10] assessed 40 models for climate studies in Australia from the CMIP5 (Coupled Model Intercomparison Project phase 5), especially in favour of application-ready data. The study selected eight models: (1) MIROC5, (2) ACCESS1-0, (3) GFDL-ESM2M, (4) HadGEM2-CC, (5) CESM1-CAM5, (6) NorESM1-M, (7) CNRM-CM5, and (8) CanESM2. Three of these eight models were recommended for representing the 'best case', 'worst case', and 'maximum consensus' scenarios for any given region, time period, and greenhouse scenario. The details of these models can be found in CSIRO and BoM [10]. In addition, SILO [40] assessed 19 climate models that were deemed to be most reliable for the Australian region. SILO [40] also provides free climate projection application-ready daily time series data under the Consistent Climate Scenarios project.

For this study, five GCMs were selected, namely ACCESS1-0, CanESM2, CNRM-CM5, GFDL-ESM2M, and MIROC5, based on the recommendation of CSIRO and BoM [12]. Furthermore, these GCMs were tested using the future climate scenarios of RCP4.5 and RCP8.5 recommended by CSIRO and BoM [10]. RCP4.5 is a medium–low stabilization scenario in which radiative forcing stabilizes at 4.5 Wm² by 2100 with a CO₂ concentration of 650 ppm. The RCP 8.5 scenario, on the other hand, is a scenario with extremely high greenhouse gas emissions and a rising radiative forcing pathway that leads to 8.5 Wm² by 2100 and a CO₂ concentration of 1370 ppm. SILO [40] provided ready to use future climate projection daily time-series data (rainfall, maximum and minimum temperature, and solar radiation) for the projection years of 2030 and 2050. These data were statistically downscaled (change factor method) using a baseline climate period of 1960 to 2010 and bias corrected with the local meteorological data.

3. Results and Discussion

3.1. Model Sensitivity and Suitability

Based on the sensitivity results, 15 streamflow parameters were ranked as very important and important as per the categorization of ranking by van Griensven et al. [41]. These were: ALPHA_BF, CANMX, CH_K2, CH_N2, CN2, EPCO, ESCO, GW_DELAY, GW_REVAP, GWQMN, SLOPE, SOL_AWC, SOL_K, SOL_Z, and SURLAG, from highest to lowest rank, respectively (please refer to Appendix A for a brief description of these parameters). Further details of these parameters can be found in Winchell et al. [32]. ParaSol (SCE-UA) auto-calibration was performed at the MYD's outlet on these 15 most sensitive streamflow parameters. Streamflow was calibrated from 1990 to 2002, during which wet,

moderate, and dry years occurred and was validated from 2003 to 2008, during which the conditions were drier and hence different to those during calibration [42,43]. In addition, the manual tuning of the SWAT model's runoff and baseflow-related parameters was performed for runoff and baseflow calibration.

The SWAT model performed very well during the calibration period for total streamflow and baseflow (daily, monthly, and annual; NSE > 0.75, $R^2 > 0.75$, RSR 0.50, and PBIAS 10%, as shown in Table 2). Similarly, the runoff calibrations (daily, monthly, and annual) were also acceptable. Although the NSE value was $0.42 < 0.50$ and the RSR value was $0.76 > 0.70$, the daily runoff calibration was deemed satisfactory as per the recommendation by Arnold et al. [44] for the daily time step (since the recommendations in Moriasi et al. [39] were for the monthly time step). During calibration, the SWAT model generally underpredicted the flows during wet periods (1990–1996) and overpredicted the flows during dry periods (1997–2002) on a monthly scale (Figure 5). Overall, during calibration, the model underpredicted the total streamflow, baseflow, and runoff (daily, monthly, and annual), as shown in Table 2, whereas the PBIAS output was positive, indicating underprediction. Furthermore, the baseflow underprediction was much lower than runoff, as shown in Table 2, where runoff PBIAS values are much higher.

Table 2. Streamflow calibration (1990–2002) and validation (2003–2008) statistics [30].

		Daily				Monthly				Annual			
		R ²	NSE	PBIAS	RSR	R ²	NSE	PBIAS	RSR	R ²	NSE	PBIAS	RSR
Total streamflow	Calibration	0.78	0.77	10	0.48	0.93	0.89	10	0.34	0.96	0.87	10	0.36
	Validation	0.74	0.72	−3	0.53	0.82	0.82	−3	0.43	0.87	0.81	−3	0.43
Baseflow	Calibration	0.90	0.87	6	0.36	0.93	0.89	6	0.33	0.95	0.88	6	0.35
	Validation	0.79	0.77	−11	0.48	0.81	0.79	−11	0.46	0.84	0.71	−11	0.54
Runoff	Calibration	0.50	0.42	23	0.76	0.84	0.80	23	0.45	0.97	0.76	23	0.49
	Validation	0.67	0.53	19	0.69	0.82	0.79	19	0.46	0.87	0.70	19	0.55

Positive and negative PBIAS values indicate underprediction and overprediction, respectively, in percent. Monthly simulations are satisfactory if NSE > 0.50, RSR ≤ 0.70, and if PBIAS ± 25% for streamflow as per Moriasi et al. [39].

During the validation period, the daily, monthly, and annual total streamflow performance ratings were also very good (NSE > 0.75, $R^2 > 0.75$, RSR 0.50, and PBIAS 10%, as shown in Table 2), despite some relaxation on the daily step guideline. Furthermore, as shown in Table 2, the validation was satisfactory in runoff and baseflow. However, as shown in Figure 5, the model overpredicted the flows in drier years (2006–2008), opposite to the comparatively wet years (2003–2005). Furthermore, the model overpredicted baseflow and total streamflow while underpredicting the runoff, as shown in Table 2, where a negative PBIAS output implies overprediction. In the validation period, the overprediction of streamflow simulation during the drier years is expected because the validation period is drier than the calibration period.

In general, the SWAT model replicated the study area well in terms of calibration and validation statistics. However, the SWAT model overpredicted and underpredicted the flows during the dry and wet periods, respectively, which was found to be consistent with the results of other SWAT studies. For example, in Australia, the SWAT model used in the Mooki catchment in NSW by Vervoort [45] overpredicted some smaller peaks and lower flows, while it underpredicted the peak runoff. In the Woody Yaloak River catchment in Victoria, the SWAT model overpredicted the low flows, as found by Watson et al. [46]. Other studies from outside Australia also had similar results. For example, the study by Green and van Griensven [47] reported overprediction and underprediction of runoff during dry and wet periods, respectively, whereas in the study by Kirsch et al. [48], the runoff was underpredicted during extremely wet years.

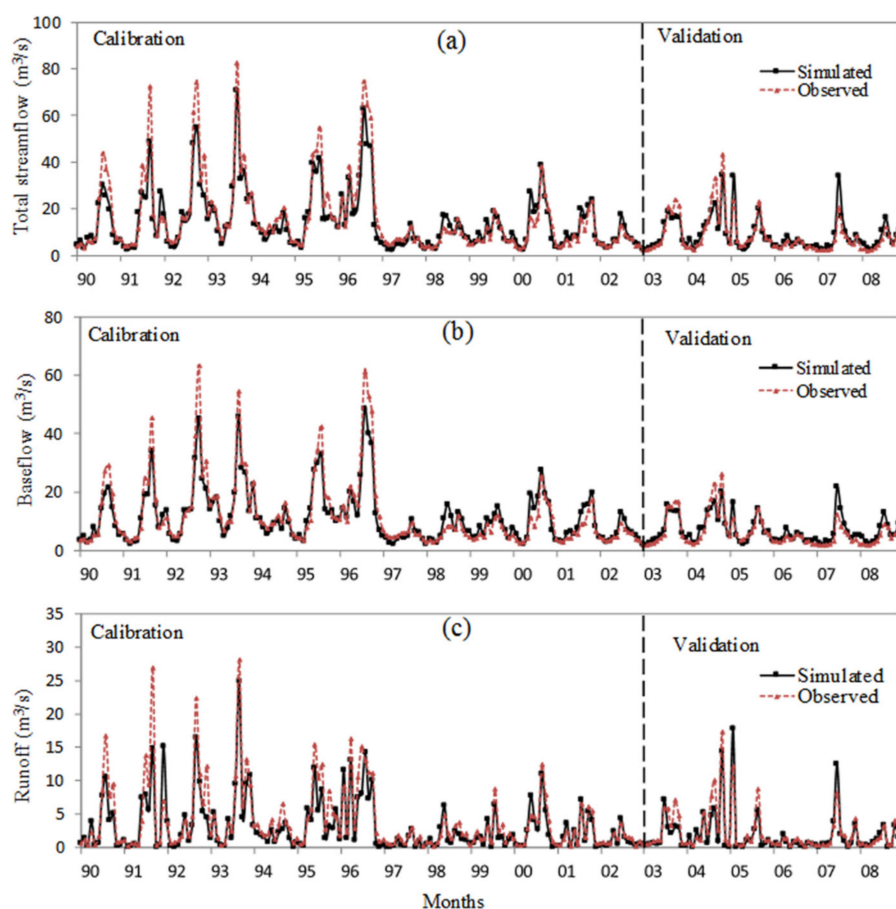


Figure 5. Comparison of observed and simulated monthly (a) total streamflow, (b) baseflow, and (c) runoff during calibration and validation in the MYD.

3.2. Climate Alteration Impacts on Future Rainfall and Temperature

Tables 3 and 4 show the rainfall and average temperature changes projected by the GCMs in 2030 and 2050, respectively, for the selected climate scenarios. In general, the cluster of scenarios for 2030 and 2050 projected rainfall reduction, except for the MIROC5 model. The highest reduction in annual rainfall was projected by the GFDL-ESM2M model as about -14% and -28% in 2030 and 2050, respectively, as shown in Tables 3 and 4. On the other hand, the cluster of scenarios for 2030 and 2050 suggested an increase in annual temperature by all models ranging between $1.1\text{ }^{\circ}\text{C}$ and $3.0\text{ }^{\circ}\text{C}$ (see Tables 3 and 4). Tables 3 and 4 also show that the changes in rainfall and temperature were not significantly different between the RCP4.5 and RCP8.5 scenarios, particularly in 2030.

The GFDL-ESM2M model projected higher variations in rainfall and temperature for the cluster of scenarios, whereas CanESM2 and MIROC5 projected lower variations in rainfall and temperature, respectively. Moreover, the reductions in rainfall were higher in the crop growing season (April to November) and more pronounced during the spring (September to November) and winter (June to August), as can be seen in Tables 3 and 4, with the highest monthly decrease of 62% by the GFDL-ESM2M model under RCP8.5 in 2050. This would have an impact on pasture productivity in the MYD. The higher increases in temperature occurred from October to December, with the highest increase of $4.2\text{ }^{\circ}\text{C}$ by the GFDL-ESM2M model under RCP8.5 in 2050.

Table 3. Change of rainfall (P, %) and temperature (T, °C) as projected by the climate models under different scenarios in 2030.

	ACCESS1-0 RCP 4.5		CanESM2 RCP 4.5		CNRM-CM5 RCP 4.5		GFDL-ESM2M RCP 4.5		MIROC5 RCP 4.5		ACCESS1-0 RCP 8.5		CanESM2 RCP 8.5		CNRM-CM5 RCP 8.5		GFDL-ESM2M RCP 8.5		MIROC5 RCP 8.5	
	P(%)	T(°C)	P(%)	T(°C)	P(%)	T(°C)	P(%)	T(°C)	P(%)	T(°C)	P(%)	T(°C)	P(%)	T(°C)	P(%)	T(°C)	P(%)	T(°C)	P(%)	T(°C)
Jan.	-1	1.2	18	1.5	-1	1.4	-3	1.3	4	1.0	-1	1.2	19	1.5	-1	1.5	-3	1.3	4	1.0
Feb.	-12	1.1	0	1.4	6	1.2	-7	1.4	0	1.0	-13	1.1	0	1.4	6	1.2	-7	1.4	0	1.0
Mar.	-13	1.4	1	1.5	-8	1.8	-3	1.3	15	0.8	-13	1.5	1	1.6	-8	1.9	-4	1.4	15	0.8
Apr.	-3	1.4	5	1.5	8	1.4	-21	1.6	15	1.3	-3	1.5	5	1.5	8	1.4	-21	1.6	15	1.3
May	-18	1.3	4	1.3	6	1.2	-11	1.2	5	1.1	-18	1.3	4	1.3	6	1.2	-11	1.3	5	1.1
Jun.	-6	1.3	-2	1.0	-9	0.9	-14	1.0	4	1.2	-6	1.3	-2	1.1	-10	0.9	-15	1.1	4	1.2
Jul.	-3	1.3	0	1.1	-9	1.0	-7	1.2	3	1.1	-3	1.3	0	1.1	-9	1.0	-7	1.2	3	1.1
Aug.	-3	1.1	-2	1.2	-9	1.0	-9	1.2	2	1.0	-3	1.2	-2	1.2	-9	1.1	-10	1.2	2	1.0
Sep.	-16	1.1	-1	1.2	-9	1.3	-25	1.2	-5	0.9	-17	1.2	-1	1.2	-10	1.4	-25	1.2	-5	0.9
Oct.	-17	1.4	-9	1.3	-15	1.4	-20	2.0	-10	1.2	-17	1.4	-9	1.3	-15	1.5	-20	2.0	-10	1.2
Nov.	-13	1.4	-12	1.6	-8	1.5	-30	2.0	1	1.2	-13	1.4	-12	1.7	-8	1.6	-31	2.1	1	1.2
Dec.	3	1.3	-4	1.8	-17	1.5	-12	1.9	-1	1.1	3	1.3	-4	1.8	-18	1.6	-13	1.9	-1	1.1
Year	-8	1.3	0	1.4	-6	1.3	-14	1.4	3	1.1	-9	1.3	0	1.4	-6	1.3	-14	1.5	3	1.1

Table 4. Change of rainfall (P, %) and temperature (T, °C) as projected by the climate models under different scenarios in 2050.

	ACCESS1-0 RCP 4.5		CanESM2 RCP 4.5		CNRM-CM5 RCP 4.5		GFDL-ESM2M RCP 4.5		MIROC5 RCP 4.5		ACCESS1-0 RCP 8.5		CanESM2 RCP 8.5		CNRM-CM5 RCP 8.5		GFDL-ESM2M RCP 8.5		MIROC5 RCP 8.5	
	P(%)	T(°C)	P(%)	T(°C)	P(%)	T(°C)	P(%)	T(°C)	P(%)	T(°C)	P(%)	T(°C)	P(%)	T(°C)	P(%)	T(°C)	P(%)	T(°C)	P(%)	T(°C)
Jan.	-2	2.1	33	2.6	-1	2.6	-6	2.3	7	1.8	-2	2.5	39	3.1	-1	3.0	-7	2.7	9	2.1
Feb.	-22	2.0	1	2.4	10	2.1	-13	2.5	0	1.7	-26	2.3	1	2.9	12	2.5	-15	2.9	1	2.0
Mar.	-23	2.5	2	2.7	-15	3.2	-6	2.4	27	1.5	-27	3.0	2	3.2	-17	3.8	-7	2.8	32	1.7
Apr.	-5	2.5	8	2.6	14	2.5	-37	2.9	27	2.3	-6	3.0	10	3.0	16	2.9	-43	3.4	32	2.7
May	-32	2.3	7	2.2	11	2.1	-19	2.2	9	2.0	-37	2.7	9	2.6	13	2.5	-23	2.6	10	2.3
Jun.	-11	2.3	-4	1.8	-17	1.6	-26	1.9	8	2.2	-13	2.7	-5	2.2	-20	1.9	-30	2.2	9	2.5
Jul.	-5	2.2	0	1.9	-16	1.8	-12	2.1	6	1.9	-6	2.6	0	2.3	-19	2.1	-15	2.5	7	2.2
Aug.	-5	2.0	-4	2.1	-16	1.8	-17	2.2	3	1.7	-5	2.4	-4	2.5	-19	2.2	-20	2.5	4	2.0
Sep.	-29	2.0	-1	2.0	-17	2.4	-44	2.1	-9	1.6	-34	2.4	-1	2.4	-20	2.8	-52	2.4	-10	1.8
Oct.	-30	2.4	-16	2.3	-26	2.5	-36	3.5	-17	2.1	-35	2.9	-19	2.7	-31	3.0	-42	4.2	-21	2.4
Nov.	-23	2.4	-21	2.9	-14	2.7	-53	3.6	1	2.1	-27	2.8	-25	3.4	-16	3.2	-62	4.2	2	2.5
Dec.	6	2.3	-7	3.2	-31	2.7	-22	3.3	-2	1.9	7	2.7	-9	3.7	-36	3.2	-26	3.9	-2	2.2
Year	-15	2.3	0	2.4	-10	2.3	-24	2.6	5	1.9	-18	2.7	0	2.8	-12	2.8	-28	3.0	6	2.2

Overall, the future climate projections indicate that the MYD will become hotter, with less winter–spring (June to November) rainfall and more droughts or water shortages in the catchment. In a similar climate change impact study for the dairy regions of Gippsland in Victoria, Hennessy et al. [49] also found a median decrease in annual rainfall of about 3% by 2040, with a range of -10% to 5% under RCP8.5. The study also expected an increase in the seasonal temperature by about 1.0 °C to 1.7 °C, with summer being the warmest and winter being the coldest. The hydrology of a catchment is greatly affected in various ways by rising temperatures and decreasing rainfalls. For example, when the temperature rises, evapotranspiration rates rise and soil moisture falls. This, in turn, increases the soil’s infiltration capacity and reduces runoff and soil erosion. Furthermore, a decline in rainfall reduces water flow, resulting in low dissolved oxygen levels.

3.3. Climate Alteration Impacts on the Hydrologic Components

The SWAT model was run with future downscaled climate data to assess the impact of climate alteration on the following hydrologic components: surface runoff, groundwater flow, evapotranspiration, soil water storage, water yield, and subsurface lateral flow. Table 5 summarizes the expected annual changes in the hydrologic components for the cluster of scenarios using the five GCM models. The annual reductions of rainfall from Tables 3 and 4 are also shown in Table 5 to correlate their effects on the water cycle components. In general, evapotranspiration (ET) and surface runoff (SURQ) changes were found to be very significant compared to other water cycle components. Moreover, there were no significant

differences in the annual percent reductions of the components between the scenarios of RCP4.5 and RCP8.5 for the same GCMs under the same projection year, as shown in Table 5.

Table 5. Change in annual hydrologic components (%) as projected by the climate models and scenarios.

Years	RCPs	GCMs	RAIN	ET	SW	SURQ	LATQ	GWQ	WYLD
2030	RCP4.5	ACCESS1-0	−8	33	−2	−84	−23	−21	−41
		CanESM2	0	40	2	−81	−12	4	−27
		CNRM-CM5	−6	34	0	−84	−19	−10	−35
		GFDL-ESM2M	−14	28	−9	−87	−32	−37	−51
		MIROC5	3	41	6	−80	−6	19	−19
	RCP8.5	ACCESS1-0	−9	33	−3	−84	−24	−22	−41
		CanESM2	0	40	2	−81	−12	4	−27
		CNRM-CM5	−6	34	−1	−84	−20	−11	−36
		GFDL-ESM2M	−14	27	−9	−87	−33	−38	−52
		MIROC5	3	42	6	−80	−6	19	−19
2050	RCP4.5	ACCESS1-0	−15	28	−11	−87	−34	−44	−54
		CanESM2	0	42	−2	−82	−15	−4	−31
		CNRM-CM5	−10	31	−6	−86	−28	−28	−46
		GFDL-ESM2M	−24	15	−21	−91	−48	−65	−68
		MIROC5	5	45	4	−79	−5	22	−17
	RCP8.5	ACCESS1-0	−18	25	−15	−88	−38	−52	−59
		CanESM2	0	43	−3	−82	−16	−7	−33
		CNRM-CM5	−12	29	−9	−87	−31	−35	−50
		GFDL-ESM2M	−28	8	−26	−93	−53	−73	−73
		MIROC5	6	46	3	−79	−5	23	−16

Note: RAIN—rainfall; ET—evapotranspiration; SW—soil water storage; SURQ—surface runoff; LATQ—lateral flow; GWQ—groundwater flow; WYLD—water yield.

Table 5 also reveals that the highest and lowest annual increases (46% and 8%, respectively) in ET occurred under the scenario of RCP8.5 in 2050 by the MIROC5 and GFDL-ESM2M models, respectively. The results also indicate that an increase in temperature and an increase or decrease in rainfall will increase evapotranspiration in the MYD, which is primarily driven by temperature. Figure 6 shows that the highest increases in monthly ET occurred in March under all MIROC5 scenarios, and it was approximately 100 percent under the extreme scenario of RCP8.5 in 2050. On the other hand, lower changes occurred in June and July. Overall, the changes in ET were significantly higher than that in other studies in Victoria, which caused a significant impact on other water cycle components, especially SURQ. For example, Hennessy et al. [49] found a median increase in ET by about 7% in all seasons with a maximum of 20% by 2030–2049 in their climate change impact study for the dairy regions of Gippsland, Victoria.

Soil water storage (SW) decreases when rainfall decreases, as shown in Table 5, which directly impacts the water cycle components, especially groundwater flow. The cluster of scenarios for 2030 and 2050 also projected significant annual reductions in SURQ with a maximum of −93% by the GFDL-ESM2M model for RCP8.5 in 2050, as shown in Table 5. Moreover, SURQ reduction in different months of the year did not vary significantly except in August, as shown in Figure 6, under the GFDL-ESM2M model scenarios. Lateral flow (LATQ) and groundwater flow (GWQ) reductions were less significant than SURQ. Moreover, annual GWQ increased when SW increased, as shown in Table 5. The MYD's annual water yield (WYLD) was expected to decrease by −16% to −73% for the cluster of scenarios where GFDL-ESM2M and MIROC5 models projected the higher and lower changes, respectively, as shown in Table 5. On the monthly scale, higher reductions in WYLD were expected to occur from October to April than from May to September, which is consistent overall with ET and SURQ, as shown in Figure 6, under all scenarios by the GFDL-ESM2M model.

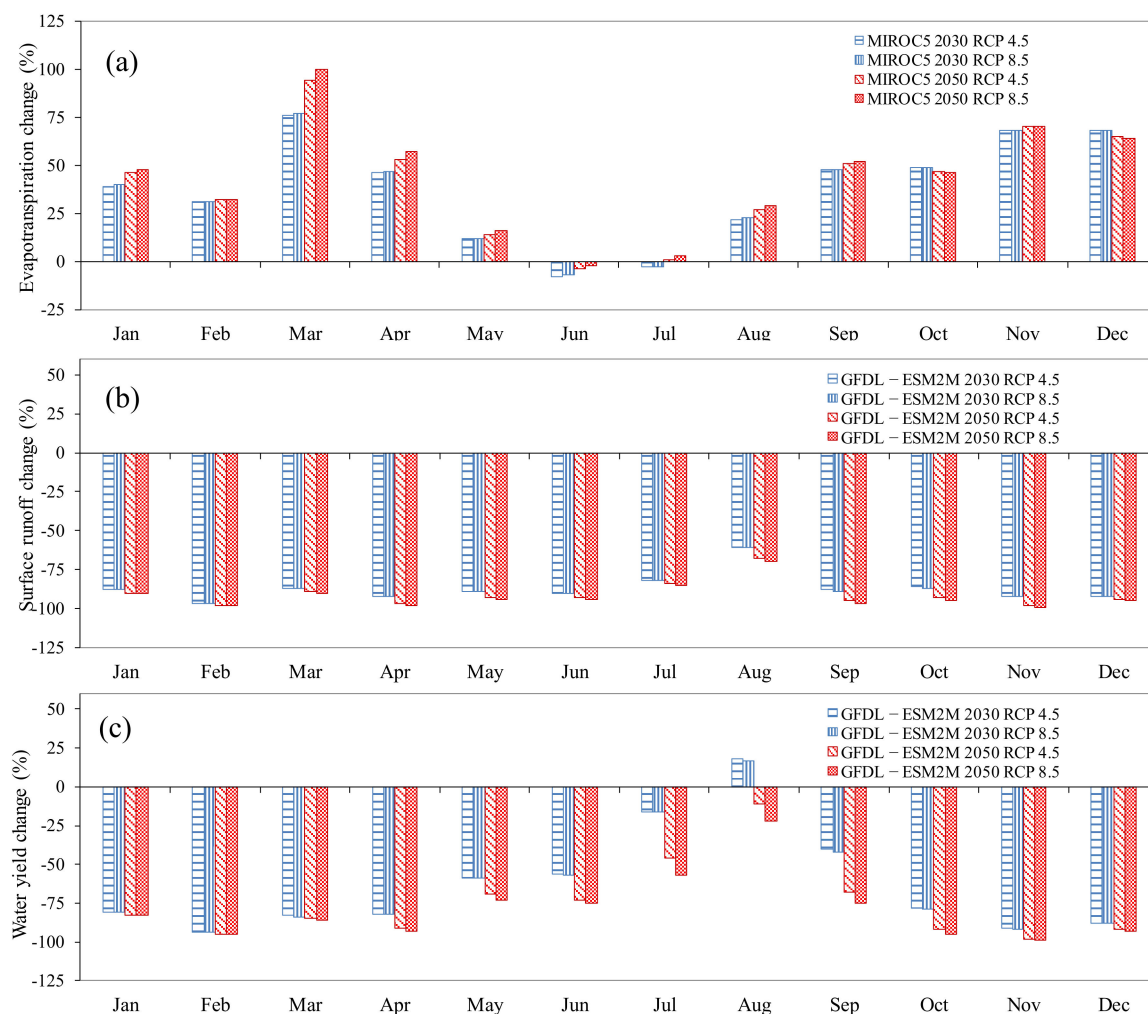


Figure 6. Changes of monthly (a) evapotranspiration, (b) surface runoff, and (c) water yield in 2030 and 2050 under the scenarios of RCP4.5 and RCP8.5.

The decrease in the yield of water and surface runoff in the study area was caused by a decrease in projected rainfall, particularly by the GFDL-ESM2M model, which is severe from the standpoint of water utilization and control because it could lead to a water scarcity problem.

4. Conclusions

Climate change-induced alterations in local rainfall and temperature may increase the risks of droughts and floods, causing a major challenge to people, societies, governments, commerce, and the environment. As a result, assessing future water resources in the context of climate alterations is critical for developing improved water management techniques and climate adaptation strategies for catchments. In this study, future climate alterations in the agricultural middle Yarra division (MYD) of the Yarra River catchment was evaluated using five CMIP5 GCMs under the RCP 4.5 and 8.5 scenarios for 2030 and 2050. These climatic scenarios were then incorporated into a calibrated SWAT model, and the alteration of future water cycle elements were described against the baseline circumstances (1990–2008).

In general, the SWAT model was found to perform well in the MYD for simulating the total streamflow (annual, monthly, and daily). The runoff and baseflow simulations were also acceptable. However, during calibration and validation, the SWAT model over-predicted and under-predicted the streamflow during dry and wet periods, respectively, which is in line with other prior studies.

The future rainfall and temperature were expected to decrease and increase, respectively, under the various climate alteration scenarios in the MYD. The highest decrease in monthly rainfall (62%) and the highest increase in monthly temperature (4.2 °C) were projected by the GFDL-ESM2M model under the scenario of RCP 8.5 in 2050. Moreover, the significant increases in future evapotranspiration (8% to 46%) greatly reduced the MYD's surface runoff, by over 80% under most of the climate scenarios.

The conclusions, limitations, and recommendations that are provided on the basis of this study are as follows:

- a. Overall, the future climate projections indicate that the MYD will become hotter, with less winter–spring (June to November) rainfall and more droughts and water shortage problems in the catchment. As a result, long-term resilience and mitigation strategies are required to address the climate alteration impact on reservoir operations and water resources within the catchment study area. Such strategies may include more tree planting, rainwater harvesting, water reclamation and recycling, and efficient irrigation.
- b. This study demonstrated that the SWAT model can be used in Australian catchments and is a useful tool for future hydro-climatic studies, considering the uncertainties, such as recording errors, and spatial and temporal discretization in the data used for the development of the SWAT model.
- c. This study was conducted only for the middle agricultural part of the Yarra River catchment, and the lower urbanized and the upper forested divisions were not included in the model due to data limitations. The authors recommend further studies to be undertaken considering the Yarra River catchment as a whole to gain a complete understanding of the future impacts of climate change on the hydrology of the catchment.
- d. This study only used ParaSol (SCE-UA), the auto-calibration method available with the SWAT modelling tool; we recommend the use of other available calibration methods, such as the SUFI-2 method recommended by Abbaspour et al. [50,51] because during the optimization process, ParaSol (SCE-UA) assumes that the model structure is correct, and the input data is free from errors.
- e. In addition, an uncertainty analysis of the SWAT model is recommended to further justify its application in Australian catchments, where available data are sparse.

Author Contributions: Conceptualization, S.K.D., M.A.U.R.T., N.M. and A.W.M.N.; methodology, S.K.D., N.M. and A.W.M.N.; validation, S.K.D., N.M., M.A.U.R.T. and A.W.M.N.; formal analysis, S.K.D.; investigation, S.K.D.; resources, S.K.D.; data curation, S.K.D.; writing—original draft preparation, S.K.D. and N.M.; writing—review and editing, S.K.D., A.A., M.H.R.B.K. and N.M.; visualization, S.K.D.; supervision, N.M. and A.W.M.N.; project administration, N.M.; funding acquisition, N.M. and A.W.M.N. All authors have read and agreed to the published version of the manuscript.

Funding: This research received no external funding.

Acknowledgments: The authors wish to acknowledge Victoria University for providing support for this study.

Conflicts of Interest: The authors declare no conflict of interest.

Abbreviations

List of Acronyms

ASC	Australian soil classification
ASTER	Advanced spaceborne thermal emission and reflection radiometer
AWBM	Australian water balance model
BoM	Bureau of Meteorology
CMIP5	Coupled Model Intercomparison Project, phase 5
CN	Curve number
CO ₂	Carbon dioxide
CSIRO	Commonwealth Scientific and Industrial Research Organisation
DEM	Digital elevation model
ET	Evapotranspiration
GCMs	General circulation models
GDEM	Global digital elevation model
IPCC	Intergovernmental Panel on Climate Change
LH-OAT	Latin-hypercube and one-factor-at-a-time
METI	The Ministry of Economy, Trade, and Industry (METI) of Japan
NASA	National Aeronautics and Space Administration
NSW	New South Wales
ParaSol	Parameter solution
PET	Potential evapotranspiration
RCP	Representative concentration pathway
SCE-UA	Shuffled complex evolution-The University of Arizona
SILO	Scientific Information for Land Owners
SUFI-2	Sequential uncertainty fitting
SWAT	Soil and water assessment tool
USDA-ARS	United States Department of Agriculture-Agricultural Research Service

Appendix A

Table A1. The streamflow parameters and their range used in the SWAT model calibration [32].

Name	Min	Max	Description
ALPHA_BF	0	1	Baseflow alpha factor (days)
CANMX	0	100	Maximum canopy storage (mm)
CH_K2	−0.01	500	Channel effective hydraulic conductivity (mm/h)
CH_N2	−0.01	0.3	Manning's <i>n</i> value for main channel
CN2	35	98	Initial SCS CN II value
EPCO	0	1	Plant uptake compensation factor
ESCO	0	1	Soil evaporation compensation factor
GW_DELAY	0	500	Groundwater delay (days)
GW_REVAP	0.02	0.2	Groundwater "revap" coefficient
GWQMN	0	5000	Threshold water depth in the shallow aquifer for flow (mm)
SLOPE	0	0.6	Average slope steepness (m/m)
SOL_AWC	0	1	Available water capacity (mm H ₂ O/mm soil)
SOL_K	0	2000	Saturated hydraulic conductivity (mm/h)
SOL_Z	0	3500	Soil depth (mm)
SURLAG	1	24	Surface runoff lag time (days)

References

1. IPCC. *Climate Change 2007: The Physical Science Basis. Contribution of Working Group I to the Fourth Assessment Report of the Intergovernmental Panel on Climate Change*; Cambridge University Press: Cambridge, UK, 2007.

2. IPCC. *Climate Change 2013: The Physical Science Basis. Contribution of Working Group I to the Fifth Assessment Report of the Intergovernmental Panel on Climate Change*; Cambridge University Press: Cambridge, UK, 2013.
3. Canadell, J.G.; Meyer, C.P.; Cook, G.D.; Dowdy, A.; Briggs, P.R.; Knauer, J.; Pepler, A.; Haverd, V. Multi-decadal increase of forest burned area in Australia is linked to climate change. *Nat. Commun.* **2021**, *12*, 6921. [[CrossRef](#)] [[PubMed](#)]
4. Daloglu, I.; Cho, K.H.; Scavia, D. Evaluating causes of trends in long-term dissolved reactive phosphorus loads to Lake Erie. *Environ. Sci. Technol.* **2012**, *46*, 10660–10666. [[CrossRef](#)] [[PubMed](#)]
5. Marshall, E.; Randhir, T. Effect of climate change on watershed system: A regional analysis. *Clim. Chang.* **2008**, *89*, 263–280. [[CrossRef](#)]
6. Tan, M.L.; Ibrahim, A.L.; Yusop, Z.; Chua, V.P.; Chan, N.W. Climate change impacts under CMIP5 RCP scenarios on water resources of the Kelantan River Basin, Malaysia. *Atmos. Res.* **2017**, *189*, 1–10. [[CrossRef](#)]
7. Samaras, A.G.; Koutitas, C.G. Modeling the impact of climate change on sediment transport and morphology in coupled watershed-coast systems: A case study using an integrated approach. *Int. J. Sediment Res.* **2014**, *29*, 304–315. [[CrossRef](#)]
8. Fowler, H.J.; Blenkinsop, S.; Tebaldi, C. Linking climate change modelling to impacts studies: Recent advances in downscaling techniques for hydrological modelling. *Int. J. Climatol.* **2007**, *27*, 1547–1578. [[CrossRef](#)]
9. Li, Z.; Fang, H. Impacts of climate change on water erosion: A review. *Earth-Sci. Rev.* **2016**, *163*, 94–117. [[CrossRef](#)]
10. CSIRO; BoM. *Climate Change in Australia Information for Australia's Natural Resource Management Regions: Technical Report*; CSIRO and Bureau of Meteorology: Melbourne, VIC, Australia, 2015. Available online: <https://www.climatechangeinaustralia.gov.au/en/publications-library/technical-report/> (accessed on 25 November 2017).
11. Potter, N.J.; Chiew, F.H.S.; Zheng, H.; Ekstrom, M.; Zhang, L. *Hydroclimate Projections for Victoria at 2040 and 2065*; CSIRO: Canberra, ACT, Australia, 2016.
12. Vaze, J.; Chiew, F.H.S.; Perraud, J.M.; Viney, N.; Post, D.; Teng, J.; Wang, B.; Lerat, J.; Goswami, M. Rainfall-runoff modelling across southeast Australia: Datasets, models and results. *Australas. J. Water Resour.* **2011**, *14*, 101–116. [[CrossRef](#)]
13. Boughton, W. The Australian water balance model. *Environ. Model. Softw.* **2004**, *19*, 943–956. [[CrossRef](#)]
14. Chiew, F.H.S.; Peel, M.C.; Western, A.W. Application and testing of the simple rainfall-runoff model SIMHYD. In *Mathematical Models of Small Watershed Hydrology and Applications*; Singh, V.P., Frevert, D.K., Eds.; Water Resources Publication: Littleton, CO, USA, 2002; pp. 335–367.
15. Letcher, R.A.; Jakeman, A.J.; Merritt, W.S.; McKee, L.J.; Eyre, B.D.; Baginska, B. *Review of Techniques to Estimate Catchment Exports*; NSW Environmental Protection Authority: Sydney, NSW, Australia, 1999.
16. Howe, C.; Jones, R.N.; Maheepala, S.; Rhodes, B. *Melbourne Water Climate Change Study: Implications of Potential Climate Change for Melbourne's Water Resources*; No. CMIT-2005-106; CSIRO and Melbourne Water: Melbourne, VIC, Australia, 2005.
17. Post, D.A.; Chiew, F.H.S.; Teng, J.; Wang, B.; Marvanek, S. *Projected Changes in Climate and Runoff for South-Eastern Australia Under 1 °C And 2 °C Of Global Warming*; A SEACI Phase 2 Special Report; CSIRO: Canberra, ACT, Australia, 2012.
18. Nguyen, H.H.; Recknagel, F.; Meyer, W.; Frizenschaf, J.; Shrestha, M.K. Modelling the impacts of altered management practices, land use and climate changes on the water quality of the Millbrook catchment-reservoir system in South Australia. *J. Environ. Manag.* **2017**, *202*, 1–11. [[CrossRef](#)]
19. Arnold, J.G.; Srinivasan, R.; Muttiah, R.S.; Williams, J.R. Large area hydrologic modeling and assessment part I: Model development. *J. Am. Water Resour. Assoc.* **1998**, *34*, 73–89. [[CrossRef](#)]
20. Borah, D.K.; Bera, M. Watershed-scale hydrologic and nonpoint-source pollution models: Review of mathematical bases. *Trans. ASAE* **2003**, *46*, 1553–1566. [[CrossRef](#)]
21. Gassman, P.W.; Reyes, M.R.; Green, C.H.; Arnold, J.G. The soil and water assessment tool: Historical development, applications, and future research directions. *Trans. ASABE* **2007**, *50*, 1211–1250. [[CrossRef](#)]
22. Ficklin, D.L.; Luo, Y.; Luedeling, E.; Zhang, M. Climate change sensitivity assessment of a highly agricultural watershed using SWAT. *J. Hydrol.* **2009**, *374*, 16–29. [[CrossRef](#)]
23. Chen, Q.; Chen, H.; Wang, J.; Zhao, Y.; Chen, J.; Xu, C. Impacts of climate change and land-use change on hydrological extremes in the Jinsha River basin. *Water* **2019**, *11*, 1398. [[CrossRef](#)]
24. Parajuli, P.B.; Jayakody, P.; Sassenrath, G.F.; Ouyang, Y. Assessing the impacts of climate change and tillage practices on stream flow, crop and sediment yields from the Mississippi River Basin. *Agric. Water Manag.* **2016**, *168*, 112–124. [[CrossRef](#)]
25. Rajib, A.; Merwade, V. Hydrologic response to future land use change in the Upper Mississippi River Basin by the end of 21st century. *Hydrol. Process.* **2017**, *31*, 3645–3661. [[CrossRef](#)]
26. Shrestha, M.K.; Recknagel, F.; Frizenschaf, J.; Meyer, W. Future climate and land uses effects on flow and nutrient loads of a Mediterranean catchment in South Australia. *Sci. Total Environ.* **2017**, *590*, 186–193. [[CrossRef](#)]
27. Sunde, M.G.; He, H.S.; Hubbart, J.A.; Urban, M.A. Integrating downscaled CMIP5 data with a physically based hydrologic model to estimate potential climate change impacts on streamflow processes in a mixed-use watershed. *Hydrol. Process.* **2017**, *31*, 1790–1803. [[CrossRef](#)]
28. Saha, P.P.; Zeleke, K. Modelling streamflow response to climate change for the Kyeamba Creek catchment of south eastern Australia. *Int. J. Water* **2014**, *8*, 241–258. [[CrossRef](#)]
29. Melbourne Water and EPA Victoria. *Better Bays and Waterways—A Water Quality Improvement Plan for the Port Phillip and Westernport Region*; Melbourne Water and EPA Victoria: Melbourne, VIC, Australia, 2009.

30. Das, S.K.; Ng, A.W.M.; Perera, B.J.C. Development of a SWAT model in the Yarra River catchment. In Proceedings of the MODSIM2013, 20th International Congress on Modelling and Simulation, Adelaide, SA, Australia, 1–6 December 2013; pp. 2457–2463, ISBN 978-0-98-721433-1. [[CrossRef](#)]
31. Das, S.K.; Ng, A.W.M.; Perera, B.J.C. Sensitivity analysis of SWAT model in the Yarra River catchment. In Proceedings of the MODSIM2013, 20th International Congress on Modelling and Simulation, Adelaide, SA, Australia, 1–6 December 2013; ISBN 978-0-98-721433-1. [[CrossRef](#)]
32. Winchell, M.; Srinivasan, R.; Di Luzio, M.; Arnold, J.G. *ArcSWAT 2.3.4 Interface for SWAT2005 User's Guide*; Grassland, Soil and Water Research Laboratory: Temple, TX, USA, 2009.
33. Borah, D.K.; Bera, M. Watershed-scale hydrologic and nonpoint-source pollution models: Review of applications. *Trans. ASAE* **2004**, *47*, 789–803. [[CrossRef](#)]
34. Isbell, R. *The Australian Soil Classification*; CSIRO Publishing: Melbourne, VIC, Australia, 2002.
35. Northcote, K.H. *A Factual Key for The Recognition of Australian Soils*, 4th ed.; Rellim Technical Publishers: Glenside, SA, Australia, 1979.
36. Arnold, J.G.; Allen, P.M.; Muttiah, R.; Bernhardt, G. Automated base flow separation and recession analysis techniques. *Ground Water* **1995**, *33*, 1010–1018. [[CrossRef](#)]
37. USDA-ARS. U.S. Department of Agriculture-Agricultural Research Service, Soil and Water Assessment Tool, SWAT: Baseflow Filter Program. 1999. Available online: <http://swatmodel.tamu.edu/software/baseflow-filter-program> (accessed on 15 November 2017).
38. Van Griensven, A. Sensitivity, Auto-Calibration, Uncertainty and Model Evaluation in SWAT2005, User Guide Distributed with ArcSWAT Program. 2005. Available online: http://biomath.ugent.be/~ann/SWAT_manuals/SWAT2005_manual_sens_cal_unc.pdf (accessed on 5 November 2017).
39. Moriasi, D.N.; Arnold, J.G.; Van Liew, M.W.; Bingner, R.L.; Harmel, R.D.; Veith, T.L. Model evaluation guidelines for systematic quantification of accuracy in watershed simulations. *Trans. ASABE* **2007**, *50*, 885–900. [[CrossRef](#)]
40. SILO. Consistent Climate Scenarios Data. 2016. Available online: <https://legacy.longpaddock.qld.gov.au/climateprojections/about.html> (accessed on 10 November 2017).
41. Van Griensven, A.; Meixner, T.; Grunwald, S.; Bishop, T.; Diluzio, M.; Srinivasan, R. A global sensitivity analysis tool for the parameters of multi-variable catchment models. *J. Hydrol.* **2006**, *324*, 10–23. [[CrossRef](#)]
42. Gan, T.Y.; Dlamini, E.M.; Biftu, G.F. Effects of Model Complexity and Structure, Data Quality, and Objective Functions on Hydrologic Modelling. *J. Hydrol.* **1997**, *192*, 81–103. [[CrossRef](#)]
43. Reckhow, K.H. Water quality simulation modelling and uncertainty analysis for risk assessment and decision making. *Ecol. Model.* **1994**, *72*, 1–20. [[CrossRef](#)]
44. Arnold, J.G.; Moriasi, D.N.; Gassman, P.W.; Abbaspour, K.C.; White, M.J.; Srinivasan, R.; Santhi, C.; Harmel, R.D.; van Griensven, A.; Van Liew, M.W.; et al. SWAT: Model use, calibration, and validation. *Trans. ASABE* **2012**, *55*, 1491–1508. [[CrossRef](#)]
45. Vervoort, R.W. Uncertainties in calibrating SWAT for a semi-arid catchment in NSW (Australia). In Proceedings of the 4th International SWAT Conference, Delft, The Netherlands, 2–6 July 2007.
46. Watson, B.M.; Selvalingam, S.; Ghafouri, M. Evaluation of SWAT for modelling the water balance of the Woody Yaloak River catchment, Victoria. In Proceedings of the MODSIM2003: International Congress on Modelling and Simulation, Townsville, QLD, Australia, 14–17 July 2003.
47. Green, C.H.; van Griensven, A. Autocalibration in hydrologic modeling: Using SWAT2005 in small-scale watersheds. *Environ. Model. Softw.* **2008**, *23*, 422–434. [[CrossRef](#)]
48. Kirsch, K.; Kirsch, A.; Arnold, J.G. Predicting sediment and phosphorus loads in the Rock River basin using SWAT. *Trans. ASAE* **2002**, *45*, 1757–1769. [[CrossRef](#)]
49. Hennessy, K.; Clarke, J.; Erwin, T.; Wilson, L.; Heady, C. *Climate Change Impacts on Australia's Dairy Regions*; CSIRO Oceans and Atmosphere: Melbourne, VIC, Australia, 2016.
50. Abbaspour, K.C.; Vejdani, M.; Haghghat, S. SWAT-CUP calibration and uncertainty programs for SWAT. In *MODSIM2007: International Congress on Modelling and Simulation*; Oxley, L., Kulasiri, D., Eds.; Modelling and Simulation Society of Australia and New Zealand: Christchurch, New Zealand, 2007; pp. 1603–1609.
51. Abbaspour, K.C.; Yang, J.; Maximov, I.; Siber, R.; Bogner, K.; Mieleitner, J.; Zobrist, J.; Srinivasan, R. Modelling Hydrology and Water Quality in the Pre-Alpine/Alpine Thur Watershed Using SWAT. *J. Hydrol.* **2007**, *333*, 413–430. [[CrossRef](#)]